Electronic Supplementary Material (ESI) for Journal of Materials Chemistry C.

Supporting information

MoS_2 nanoflowers and gold nanoparticles modified surface plasmon resonance biosensor for sensitivity-improved immunoassay

Peili Zhao[1,2,5], Yaofei Chen[2,5], Yu Chen[2], Shiqi Hu[2], Hui Chen[3], Wei Xiao[3], Guishi Liu[2], Yong Tang[3], Jifu Shi[4], Zhendan He[1], Yunhan Luo[2*], Zhe Chen[2]*

[1] Guangdong Key Laboratory for Genome Stability & Human Disease Prevention, School of Pharmaceutical Sciences, Shenzhen University Health Science Center, Shenzhen 518055, China

[2] Key Laboratory of Optoelectronic Information and Sensing Technologies of Guangdong Higher Education Institutes, Jinan University, Guangzhou, 510632, China

[3] Department of Bioengineering, Guangdong Province Engineering Research Center for antibody drug and immunoassay, Jinan University, Guangzhou 510632, China

[4] Siyuan Laboratory, Department of Physics, Jinan University, Guangzhou 510632, China

[5] The authors contribute equally to this work.

* Corresponding authors: Zhendan He, hezhendan@szu.edu.cn; Yunhan Luo, yunhanluo@163.com

Key words: Surface plasmon resonance, biosensor, sensitivity improvement, MoS_2 nanoflowers, gold nanoparticles

1. Experimental setup

All the measurements were carried out by a homemade SPR testing system based on the Kretchmann configuration as shown in **Figure S1**. The fabricated SPR sensor can be mounted on the prism (with the same material of slide, namely K9 glass) with the aid of index-matching liquid (cedar oil) for test. The incident light, emitted from a tungsten-halogen lamp light source [AvaLight-HAL-(S)-Mini, China], propagates through a piece of multimode fiber and is collimated by an objective lens and a convex lens. A polarizer is used to generate the transverse-magnetic wave, which then illuminates the gold film and excites the surface plasmon wave at a specific wavelength if the wave vectors of the light and surface plasmon wave are matched. Then, the output light is recorded by a spectrometer (AvaSpec-ULS2048XL, China) with the aid of a convex lens and object lens. The measured data are finally sent to a computer for further processing. Because of the SPR phenomenon, the transmittance spectrum features an absorption dip and its location is sensitive to the surrounding RI or the binding of antigen-antibody on the surface of sensor. Therefore, the sensing to bulk refractive index (RI) or the analyte concentration can be realized by tracking the location of dip, namely the resonance wavelength.

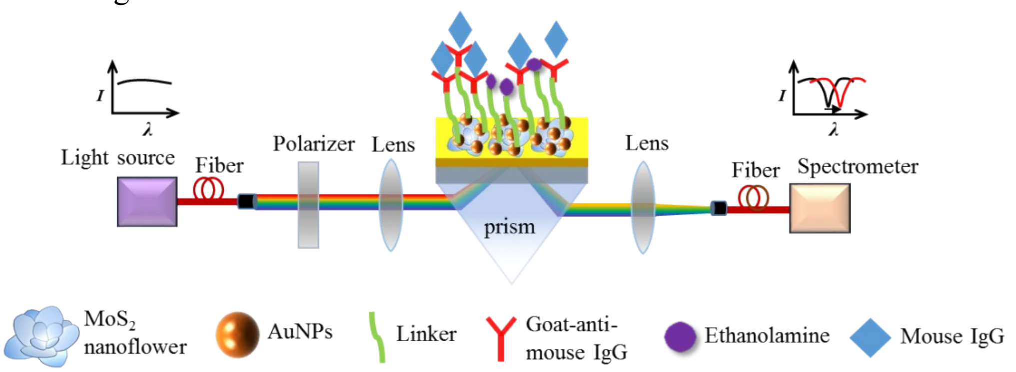

Figure S1. Schematic diagram of the experimental setup.

2. Measured results for bulk RI sensing

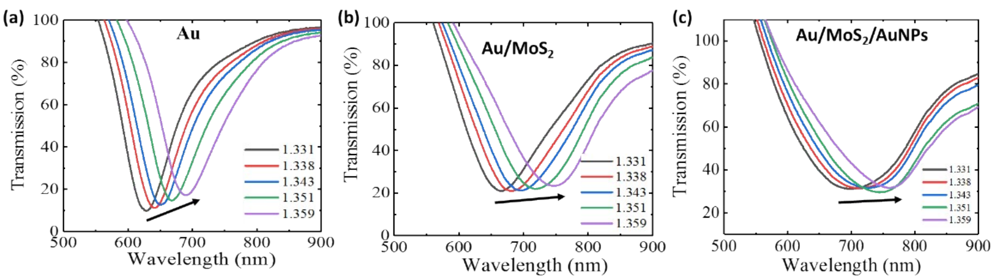

Figure S2. The transmission spectra of (a) the bare SPR sensor, (b) the MoS_2-deposited SPR sensor, and (c) the MoS_2-AuNPs-deposited sensor, under different RIs. In (c), the averaged diameter of the used AuNPs is 16 nm.

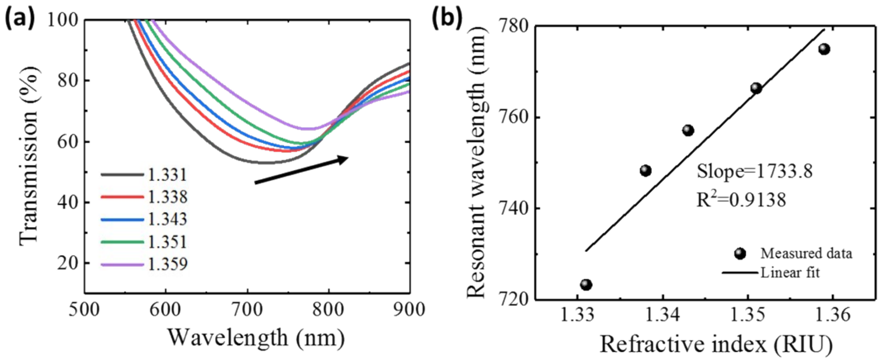

Figure S3. For the MoS_2-AuNPs-deposited sensor using the 30 nm AuNPs, (a) the transmission spectra, and (b) the resonant wavelength depending on the RI.

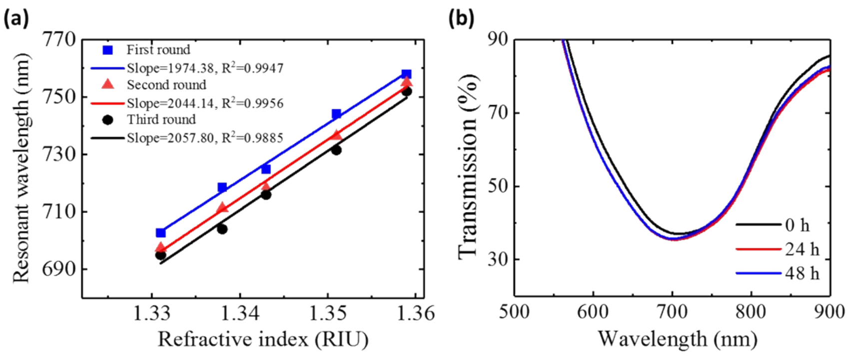

Figure S4. (a) RI sensitivities obtained by measuring for three rounds immediately. (b) Transmission spectra under the RI of 1.331 measured for three times with 24 hour intervals. Note that the tested MoS_2-AuNPs-modified sensors in (a) and (b) are two different ones.

3. Simulation

3.1 Simulation method

The transmission spectra and the corresponding electric field distributions at the resonant wavelengths were simulated by the transfer matrix method (TMM) [1] and the finite-difference time domain method (Lumerical FDTD solution), respectively. During simulation, the RI of prism (K9 glass) was set as 1.5163, and the dispersion relationships of MoS_2 was referred to the published data [2], and the "Au (Gold) - CRC" provided in the materials database of Lumerical FDTD solution was employed for the dispersion relationship of gold. The thickness of gold layer was set as 50 nm, and the Cr layer (only ~5nm) was ignored for simplification. The incident light was a p-polarized plane wave, namely the polarization direction being parallel to the incident plane, and its incident angle was set as 74°.

Because of the porous and bumpy morphology of the MoS_2 nanoflowers or the MoS_2/AuNPs layer modified on the gold film as shown in **Figure 2**a and **Figures 6**b-6d, the RI solution will fill the vacancy of the modification layer. Therefore, it is reasonable to consider the MoS_2 nanoflowers or the MoS_2/AuNPs layer and the surrounding RI solution together as an effective dielectric layer (EDL). Due to the similar reason, the antibody-antigen layer together with the surrounding RI solution can also be considered as an EDL. The effective RI n_{eff} of the EDL can be described as [3, 4]

$$n_{eff} = n_{mod} f_{mod} + n_{sol} f_{sol} \quad (1)$$

where n_{mod} and n_{sol} are the refractive indices of the modification layer and the bulk RI solution, respectively; f_{mod} and f_{sol} are the corresponding occupation ratios in volume, and $f_{mod} + f_{sol} = 1$. In our case, the modification layer can be the MoS_2 nanoflowers layer, the MoS_2/AuNPs layer, and the antibody-antigen layer, which are termed as EDL_1, EDL_2, and EDL_3 (or EDL_4), respectively, as shown in **Figure S5**. The n_{sol} is fixed as 1.333, namely RI of DI water.

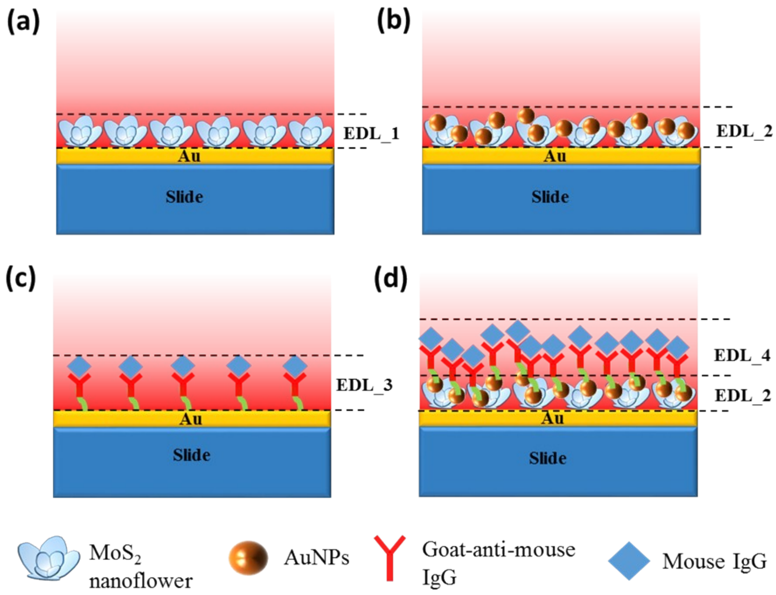

Figure S5. The schematic diagrams of the (a) EDL_1 - MoS_2 nanoflowers layer, (b) EDL_2 - MoS_2/AuNPs layer, (c) EDL_3 - antibody-antigen layer, and (d) EDL_4 - antibody-antigen layer on the EDL_2.

3.2 Bulk RI sensing

First, the simulations for bulk RI sensing were conducted. The simulated transmission spectra are shown in **Figure S6**a, where the thicknesses of the MoS_2 and MoS_2/AuNPs modification layers, namely the thicknesses of EDL_1 and EDL_2, were set as 10 and 20 nm, and the corresponding f_{mod} were set as 0.1 and 0.2, respectively. We can see the simulated spectra agree well with the measured ones shown in **Figure 3**a. It is worth noting that the thicknesses of hybrid dielectric (tens of nanometers) employed in simulation are much smaller than the marked value of 376 nm shown in **Figure 6**d. This is based on the fact that the marked thickness is the largest one presented in the SEM picture, and it is actually much larger than the average thickness of the overlayer, because the overlayer features with the porous morphology **Figures 6**b-6c.

Based on the simulated spectra, we can obtain the resonant wavelengths (624, 669, 713 nm) from **Figure S6**a. Then, electric filed distributions at these resonant wavelengths were simulated by FDTD. In the simulation, the mesh grid of the gold film and overlayer was set as 1 nm, while the default mesh was used for the remained simulation region. The Bloch and PML boundary conditions were applied to the boundaries of the simulation region. The results (**Figure S6**b) show that the addition of MoS_2 can enhance the electric field on the surface of sensor, but the further addition of AuNPs leads to the significant weakening of the amplitude of electric field. This is consistent with and can explain the change trend of the sensitivity to bulk RI shown in **Figure 3**b, because the amplitude of electrical field is proportional to the overlap integral between the evanescent field and the analyte, namely the sensitivity.

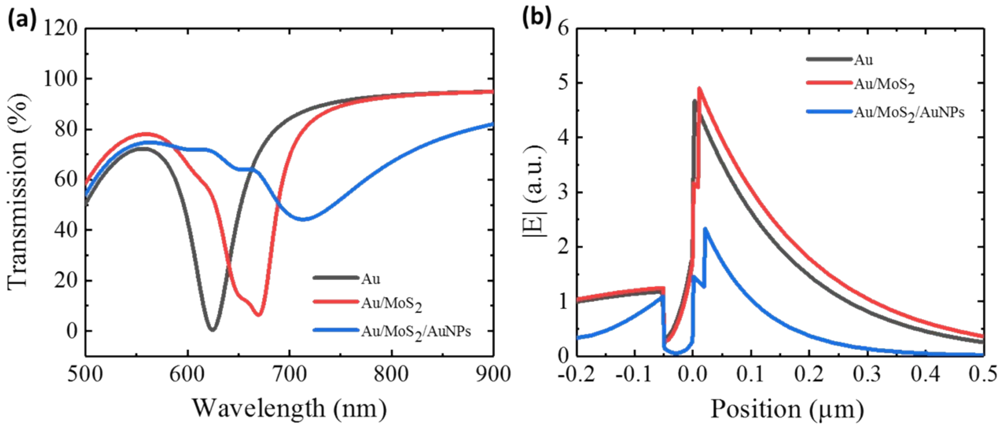

Figure S6. (a) The simulated transmission spectra of the sensors under the bulk RI of 1.333. (b) The electric field in the vicinity of the surface of sensor.

3.3 IgG sensing

In the simulation for IgG sensing, the EDL_3 and EDL_4 are added onto the surfaces of the Au film and the Au/MoS_2/AuNPs, respectively, as shown in **Figures S5**c and **S5**d. Here, the RIs of the IgG-antibody and IgG are all set as 1.5.[5]

Considering the IgG molecular dimensions of 13.7nm×8.4nm (width×height) [6],

we choose the simplified 20 nm as the thickness of the EDL_3 and EDL_4, namely the IgG antibody-antigen layer. Then, using the effective RI equation (1) and the TMM, we can simulate the transmission spectra before and after the addition of EDL_3 and EDL_4 onto the Au surface and EDL_2, and the results are shown in **Figure S7**. Here, the f_{mod} for EDL_3 is set as 0.22 to meet the wavelength shift amount 11.9 nm measured by experiment after the addition of IgG antibody-antigen layer. From **Figure S7**, we can see that if the f_{mod} of EDL_4 is set as 0.22 too, the simulated wavelength shift amount of 10.5 nm is significantly smaller than the measured 24.7 nm by experiments. The really measured 24.7 nm can only be met by increasing the f_{mod} to 0.52, indicating that the amount of antibodies modified on the surface of MoS_2/AuNPs layer is larger than that on the flat Au film surface. The increment of the antibodies amount is estimated to be ~2.4 times.

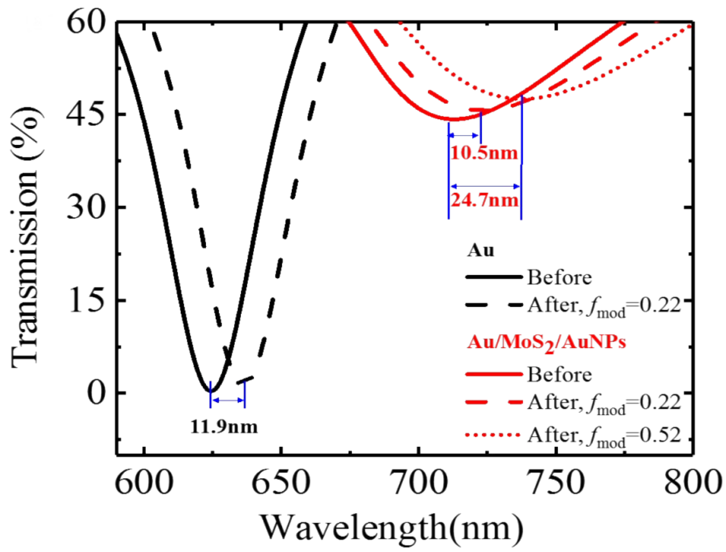

Figure S7. Simulated transmission spectra before and after the addition of the EDL_3 and EDL_4 on the Au surface and the Au/MoS_2/AuNPs surface, respectively.

4. Roughness evaluation

To evaluate the roughness of the modified surface, we extracted the height information of the modified layer from the TEM image of the cross section of the sensor's interface shown in **Figure 6**d. Ninety-one data were totally obtained and presented in **Figure** S8. The roughness average (RA) value, which is the key index to characterize the surface roughness, can be calculated by the following equation:

$$RA = \frac{1}{N}\sum_{i=1}^{N}\left|H_i - H_{\text{mean}}\right| \tag{2}$$

where N is the number of sampled points, namely 91; H_i is the height value of the ith point, and H_{mean} is the average height (286.94 nm) of all the sampled points. As a result, the RA of the modified surface is calculated as 41.4 nm.

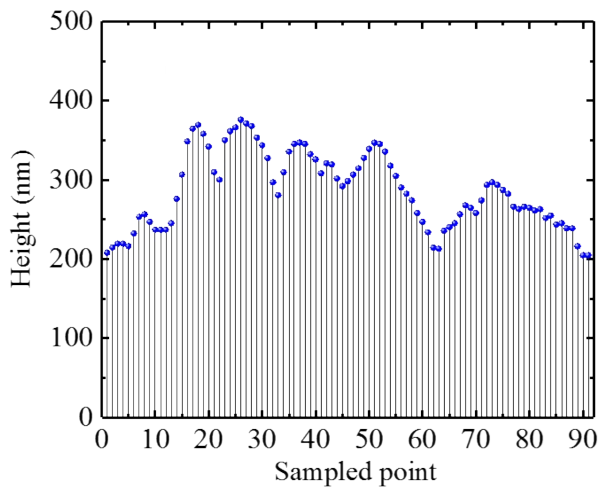

Figure S8. The heights of the modified layer at the sampled points extracted from the Figure 6d.

References

1. A. K. Mishra, S. K. Mishra, and R. K. Verma, "Graphene and beyond graphene MoS2: a new window in surface-plasmon-resonance-based fiber optic sensing," The Journal of Physical Chemistry C **120**, 2893-2900 (2016).
2. H. L. Liu, C. C. Shen, S. H. Su, C. L. Hsu, M. Y. Li, and L. J. Li, "Optical properties of monolayer transition metal dichalcogenides probed by spectroscopic ellipsometry," Appl. Phys. Lett. **105**, 201905 (2014).
3. Y. Chen, S. Hu, H. Wang, Y. Zhi, Y. Luo, X. Xiong, J. Dong, Z. Jiang, W. Zhu, and W. Qiu, "MoS2 Nanosheets Modified Surface Plasmon Resonance Sensors for Sensitivity Enhancement," Advanced Optical Materials **7**, 1900479 (2019).
4. J. Zhu, Y. Ke, J. Dai, Q. You, L. Wu, J. Li, J. Guo, Y. Xiang, and X. Dai, "Topological insulator overlayer to enhance the sensitivity and detection limit of surface plasmon resonance sensor," Nanophotonics (2019).
5. D. S. Wang, C. C. Chang, S. C. Shih, and C. W. Lin, "An ellipsometric study on the density and functionality of antibody layers immobilized by a randomly covalent method and a protein a-oriented method," Biomedical Engineering: Applications, Basis and Communications **21**, 303-310 (2009).
6. Y. H. Tan, M. Liu, B. Nolting, J. G. Go, J. Gervay-Hague, and G.-y. Liu, "A nanoengineering approach for investigation and regulation of protein immobilization," ACS nano **2**, 2374-2384 (2008).